

## Comparison of the Electronic Structures of Imine and Hydrazone Side-Chain Functionalities with the Aid of $^{13}\text{C}$ and $^{15}\text{N}$ NMR Chemical Shifts and PM3 Calculations. The Influence of C=N-Substitution on the Sensitivity to Aromatic Substitution

K. Neuvonen,<sup>\*,†</sup> F. Fülöp,<sup>‡</sup> H. Neuvonen,<sup>†</sup> A. Koch,<sup>§</sup> E. Kleinpeter,<sup>§</sup> and K. Pihlaja<sup>†</sup>

Department of Chemistry, University of Turku, FIN-20014 Turku, Finland, Institute of Pharmaceutical Chemistry, University of Szeged, H-6701 Szeged, POB 121, Hungary, and Department of Chemistry, University of Potsdam, D-14415 Potsdam, POB 691553, Germany

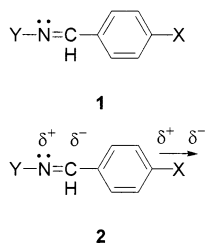
kari.neuvonen@utu.fi

Received September 16, 2002

Benzaldehyde derivatives possessing a C=N double bond in the side-chain of the aromatic ring exhibit a reverse dependence of the  $^{13}\text{C}$  NMR chemical shifts of the C=N carbon on the benzyldenic substituents X. Thus, electron-withdrawing substituents cause shielding (shift is reduced), while electron-donating ones cause deshielding. The origin of this phenomenon, which is in contrast with the idea of the generalized electronic effect, is extensively studied here by comparing the behavior of sets of benzaldehyde derivatives bearing various substituents Y on the C=N nitrogen (Y-N=CH-C<sub>6</sub>H<sub>4</sub>-X). The effects of substituents X on the C=N unit change when Y is varied. Combination of the influences of the substituents X and Y gives a sensitive balance between the different resonance structures of the compounds. Our graphical treatment, where the  $\rho_I$  and  $\rho_R$  values observed for substituent X are plotted against the  $\sigma_p^+$  value of substituent Y, is a novel use of Hammett-type substituent parameters. The justification of this method and our conclusions could be verified, for instance, by the fair correlation between the  $\rho_I$  or  $\rho_R$  values and the atomic charges of the imine carbon of the unsubstituted phenyl derivatives as well as by the correlations of the relevant bond orders and/or bond lengths both with the substituent parameters and with the atomic charges.

### Introduction

The medicinal importance of hydrazones is well established. However, as compared with azomethines, the electronic effects prevailing in the -N=N=CH- functionality and the sensitivity of these effects to substitution are not satisfactorily understood.



Extensive  $^{13}\text{C}$  NMR spectroscopic and theoretical calculation data together demonstrate that the C=N carbon of azomethines **1** derived from substituted benzaldehydes behaves normally and is shielded (shift is reduced) with increasing electron density on the carbon in question.<sup>1a</sup> In contrast, the atomic charge displays a reverse depen-

dence on substitution, i.e., electron-withdrawing phenyl substituents increase the electron density on the C=N carbon.<sup>1a</sup> As a consequence, the imine carbon resonance reveals a reverse behavior as concerns substitution: *electron-withdrawing substituents cause shielding*. In principle, the substituent-induced changes in the chemical shift, SCS, depend on the inductive ( $\sigma_I$  or  $\sigma_F$ ) and resonance ( $\sigma_R$ ) parameters according to eq 1:

$$\text{SCS} = \rho_I \sigma_I \text{ (or } \rho_F \sigma_F) + \rho_R \sigma_R \quad (1)$$

where SCS is the  $^{13}\text{C}$  NMR shift for a substituted compound relative to that for the unsubstituted one. With imines, a better correlation is obtained with this dual-substituent parameter (DSP) approach than with any of the single-parameter equations tested ( $\sigma$ ,  $\sigma^+$ ,  $\sigma^-$ ,  $\sigma_I$ ,  $\sigma_F$ ), but the small values of  $\rho_R$  show that resonance factors are not of great importance.<sup>1a</sup> The  $\rho_I/\rho_F$  values range from -3 to -4, while the  $\rho_R$  values range only from -0.7 to 0.2.

For imines, the charge on the C=N carbon and that on the C=N nitrogen behave inversely.<sup>1a</sup> This suggests

(1) (a) Neuvonen, K.; Fülöp, F.; Neuvonen, H.; Koch, A.; Kleinpeter, E.; Pihlaja, K. *J. Org. Chem.* **2001**, *66*, 4132. (b) Neuvonen, H.; Neuvonen, K. *J. Chem. Soc., Perkin Trans. 2* **1999**, 1497. (c) Neuvonen, H.; Neuvonen, K.; Koch, A.; Kleinpeter, E.; Pasanen, P. *J. Org. Chem.* **2002**, *67*, 6995.

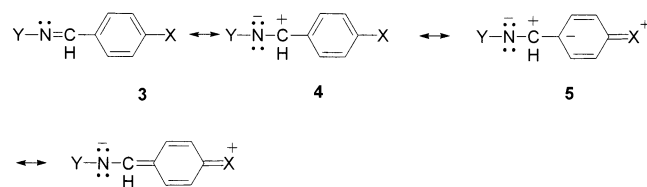
\* Corresponding Author. Fax: +358-2-3336700.

<sup>†</sup> University of Turku.

<sup>‡</sup> University of Szeged.

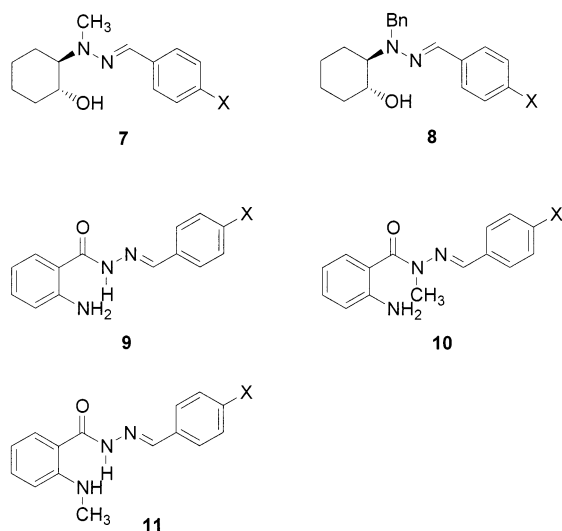
<sup>§</sup> University of Potsdam.

## SCHEME 1



substituent-induced polarization of the C=N unit, i.e.,  $\pi$ -polarization (**2**) and/or inherent polarization (Scheme 1). The concept of  $\pi$ -polarization has been extensively discussed in the literature.<sup>2–5</sup> According to this idea, the substituent dipole polarizes each  $\pi$ -unit as a localized system, as shown in **2**.  $\pi$ -Polarization has been used to explain the reverse behavior of the <sup>13</sup>C NMR chemical shifts of sp<sup>2</sup> or sp hybridized carbons in several different systems.<sup>2,5–7</sup> The idea of  $\pi$ -polarization has also been criticized, but without any explanation for the reverse behavior of the carbon shifts.<sup>8</sup> However, we recently proposed an alternative mechanism to account for the behavior of unsaturated aromatic side chains.<sup>1</sup>

The substituent-sensitive inherent polarization of the –C=N– unit (Scheme 1) of imines was proposed as an alternative/competitive explanation for  $\pi$ -polarization. The inductive and resonance effects of substituents X on the stabilities of the different resonance forms **3–6** were then considered.<sup>1a</sup> According to this concept, electron-withdrawing substituents decrease the contribution of the polarized form **4** through inductive destabilization, increasing the electron density on the C=N carbon as a consequence, while electron-donating substituents have an opposite effect, with negative  $\rho_F$  values as a result. Conjugative effects of the substituents seem to be negligible.<sup>1a</sup> The small negative  $\rho_R$  values were explained by resonance-induced polar effects (see structure **5**).



X = NO<sub>2</sub>; CN; CF<sub>3</sub>; F; Cl; Br; H; Me; OMe; or NMe<sub>2</sub>

(2) Craik, D. J.; Brownlee, R. T. C. *Prog. Phys. Org. Chem.* **1983**, *14*, 1.

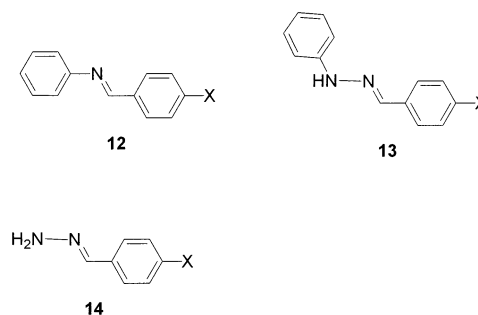
(3) Reynolds, W. F. *Prog. Phys. Org. Chem.* **1983**, *14*, 165.

(4) (a) Hamer, G. K.; Peat, J. R.; Reynolds, W. F. *Can. J. Chem.* **1973**, *51*, 897. (b) Hamer, G. K.; Peat, J. R.; Reynolds, W. F. *Can. J. Chem.* **1973**, *51*, 915.

The reverse dependence of the C=N carbon <sup>13</sup>C NMR chemical shift on phenyl substitution has previously been observed in this laboratory not only for imine structures<sup>1a</sup> but also for hydrazones **7–11**.<sup>6,7</sup> In all cases, the C=N shift correlated poorly with Hammett-type single-parameter equations but well with a DSP equation. Differing from imines, both inductive and resonance contributions are highly significant for hydrazones.<sup>6,7</sup> In the present work, we have focused on the characterization of the origin of the differences in substituent dependence of the C=N carbon resonances of imines and hydrazones. A further goal was to investigate more generally the influence of the substituent (Y) on the C=N nitrogen (Y–N=CH–) on the sensitivity of the –C=N carbon resonance to the phenyl substituent X (–N=CH–C<sub>6</sub>H<sub>4</sub>–X).

## Results

We performed <sup>15</sup>N NMR measurements on the hydrazone series **7** and **10**, for which the <sup>13</sup>C NMR data exist in our previous work,<sup>6,7</sup> and also on the imine series **12**. For the latter series, the <sup>13</sup>C NMR shifts were also recorded. Additionally, we report the PM3 atomic charges and bond lengths for the same compounds and also for hydrazones **13** and **14**.



For series **13** and **14**, the literature NMR data were used.<sup>9,12</sup> The NMR and atomic charge data are given in Supporting Information in Tables S2–S6. The bond length data are collected in Supporting Information in Table S7 and bond lengths for some relevant compounds are given in Table 4.

## Discussion

Table 1 includes  $\rho_I$  or  $\rho_F$  and  $\rho_R$  values for imines and hydrazones, determined in our previous works<sup>1a,6,7</sup> or in this study, or values either found in the literature<sup>5</sup> or calculated by us using <sup>13</sup>C NMR chemical shifts observed earlier.<sup>6,7,9</sup> Both the inductive and resonance correlation

(5) Bromilow, J.; Brownlee, R. T. C.; Craik, D. J.; Fiske, P. R.; Rowe, J. E.; Sadek, M. *J. Chem. Soc., Perkin Trans. 2* **1981**, 753.

(6) Neuvonen, K.; Fülöp, F.; Neuvonen, H.; Pihlaja, K. *J. Org. Chem.* **1994**, *59*, 5895.

(7) Neuvonen, K.; Fülöp, F.; Neuvonen, H.; Simeonov, M.; Pihlaja, K. *J. Phys. Org. Chem.* **1997**, *10*, 55.

(8) Dahn, H.; Carrupt, P.-A. *Magn. Reson. Chem.* **1997**, *35*, 577.

(9) Gordon, M. S.; Sojka, S. A.; Krause, J. G. *J. Org. Chem.* **1984**, *49*, 97.

(10) Arrowsmith, J. E.; Cook, M. J.; Hardstone, D. J. *Org. Magn. Reson.* **1978**, *11*, 160.

(11) Hansch, C.; Leo, A.; Taft, R. W. *Chem. Rev.* **1991**, *91*, 165.

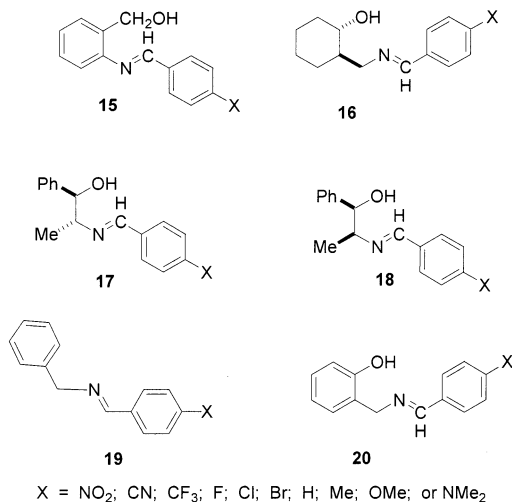
(12) Westerman, P. W.; Bottto R. E.; Roberts, J. D. *J. Org. Chem.* **1978**, *43*, 2590.

**TABLE 1.**  $\rho_I/\rho_F$  and  $\rho_R$  Values Obtained by DSP Treatment of the C=N Carbon  $^{13}\text{C}$  NMR Chemical Shifts in  $\text{CDCl}_3$  for the *para*-Substituted Imine Series 12 and 15–19 and for the Hydrazone Series 7–11, 13, and 14

line	series	$\rho_I$ or $\rho_F$	$\rho_R$	shift range	ref
1	15	-3.7	-0.1	157.16–159.99	1a
2	16	-3.0	0.2	158.79–160.80	1a
3	17	-3.6	-0.5	159.43–161.93	1a
4	18	-3.2	-0.1	158.39–160.57	1a
5	12	-4.0	-0.7	157.33–160.34	this work
6	19	-3.6	-0.7	159.8–162.03	5 <sup>a</sup>
7	13	-4.6	-3.1	133.75–138.64	6 <sup>b</sup>
8	14	-5.5	-2.7	138.55–143.26	6 <sup>b</sup>
9	7	-6.2	-4.9	127.14–133.93	6
10	8	-5.8	-5.0	127.46–134.34	6
11	9	-4.2	-2.0	144.4–148.5	7
12	10	-4.6	-1.8	135.8–140.4	7
13	11 <sup>c</sup>	-3.8	-1.6	144.1–147.9	7

<sup>a</sup>  $^{13}\text{C}$  NMR data from ref 10. <sup>b</sup>  $^{13}\text{C}$  NMR data from ref 9. <sup>c</sup> In  $\text{DMSO}-d_6$ .

parameters of the hydrazones are higher than those observed for the imines. The significantly higher contribution of resonances with negative  $\rho_R$  values for the hydrazones is especially noteworthy. The results indicate the higher sensitivity of the polarization of the C=N unit of the hydrazones to substitution as compared with that of the imines or higher shift:charge ratios for the former compounds. Moreover, the C=N carbon resonances of the hydrazones appear at a field higher by ca. 15–30 ppm than those for the imines.



**Atomic Charges vs Substituent Parameters.** To assess the effect of substituents on the polarization of the C=N unit, the variation of the atomic charges was studied. Table 2 reports the statistical results for the correlations of the calculated charges of the C=N carbon and the C=N nitrogen and N2 of the hydrazone series 7, 10, 13, and 14, for the C=N carbon and C=N nitrogen of the imine series 12, and for comparison, also those calculated previously<sup>1a</sup> for the imine series 15 and 20, with the substituent parameters  $\sigma$  and  $\sigma^+$ . In all cases, the correlation with  $\sigma$  is better than that with  $\sigma^+$ . The slopes for the C=N carbon charges are negative in all cases. This means reverse behavior, i.e., the electron density on the C=N carbon increases, although the electron-withdrawing ability of the substituent, measured

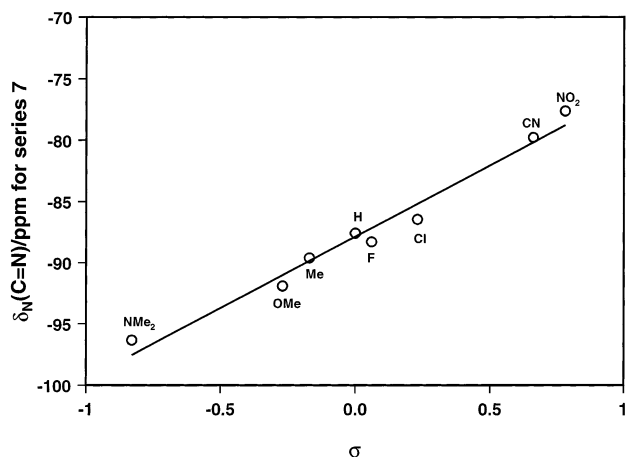


**FIGURE 1.** Plot of the  $^{15}\text{N}$  NMR chemical shifts of the C=N nitrogen for series 7 in  $\text{CDCl}_3$  vs Hammett substituent constants  $\sigma$ .

by  $\sigma/\sigma^+$ , increases. The  $q_{\text{C}}(\text{C}=\text{N})$  values of the hydrazones (Table 2; slopes  $-0.044$ ,  $-0.032$ ,  $-0.046$ , and  $-0.043$  for lines 15, 26, 37, and 47, respectively) possess a clearly higher sensitivity toward substitution than do the  $q_{\text{C}}(\text{C}=\text{N})$  values of the imines ( $-0.027$ ,  $-0.029$ , and  $-0.026$  for lines 1, 5, and 9, respectively). In contrast with the reverse behavior of the C=N carbon, the slopes for the correlations of the charges of the C=N nitrogen or N2 are positive in all cases (lines 3, 7, 11, 18, 20, 29, 39, 41, 49, and 51), with the exception of the charge of N2 of 2-aminobenzoylhydrazones 10. In the latter case, negative slopes are obtained for both  $\sigma$  and  $\sigma^+$  correlations (lines 31 and 32), but the values are so small that they in fact indicate that the atomic charge on N2 does not depend on the phenyl substituent. For the other series studied, the electron density on both nitrogens decreases when the phenyl substituents become more electron-withdrawing,  $q_{\text{N}}(\text{C}=\text{N})$  being about 2–3 times as sensitive to substitution as  $q_{\text{N}}(\text{N}2)$ . For *N*-2-hydroxycyclohexyl-*N*-methylhydrazones 7, the slope of the  $q_{\text{N}}(\text{C}=\text{N})$  vs  $\sigma$  plot (0.030) is not significantly higher than the corresponding slopes for the imines 15, 20, and 12 (0.029, 0.026, and 0.024, respectively). For the other hydrazones, 10, 13, and 14, the corresponding slopes, 0.023, 0.023, and 0.026, respectively, are almost the same as those observed for the imines.

**$^{15}\text{N}$  NMR Shifts of Imines and Hydrazones.** The C=N nitrogen of the imine series 12 resonates at a field higher by ca. 42–74 ppm than that for the reference nitromethane. The C=N nitrogen of series 7 and 10 resonates at a field higher by ca. 78–96 ppm and 42–66 ppm, respectively, and N2 at a field higher by ca. 304–319 ppm and 210–213 ppm, respectively, than that for the reference nitromethane. The  $^{15}\text{N}$  NMR shifts for the C=N nitrogen of 7 and 10 correlate well with the substituent constants  $\sigma$  (Table 2; lines 22 and 33) with slopes of ca. 12 and 15, respectively (cf. Figures 1 and S1). The N2 resonance is less sensitive. For 7 and 10, the slopes are ca. 9 (line 24) and 2.3 (line 35), respectively, and the correlation is only moderate in both cases (cf. Figures 2 and S2). The slope values for hydrazones, 12 and 15, are clearly smaller than the corresponding slope of ca. 20 for the C=N nitrogen of the *N*-benzylidene-anilines (12) (line 13). On the other hand, the slopes of

**TABLE 2. Statistical Data for Hammett-type Correlations of Atomic Charges on C=N Carbons and C=N Nitrogens or N2 for Imine Series 12, 15, and 20 and for Hydrazone Series 7, 10, 13, and 14 (Correlations of  $\delta_N(\text{C=N})$  and  $\delta_N(\text{N2})$  Values with  $\sigma$  or  $\sigma^+$  for Series 7, 10, 12, and 13 Are Also Included)<sup>a</sup>**

line	series	type of compound	correlation	slope $\pm s$	$r$	ref	
1	15 <sup>b</sup>	imine	q <sub>C</sub> (C=N) vs $\sigma$	-0.027 $\pm$ 0.004	0.9389	1	
2	15 <sup>b</sup>		q <sub>C</sub> (C=N) vs $\sigma^+$	-0.017 $\pm$ 0.003	0.9002	1	
3	15		q <sub>N</sub> (C=N) vs $\sigma$	0.026 $\pm$ 0.003	0.9466		
4	15		q <sub>N</sub> (C=N) vs $\sigma^+$	0.016 $\pm$ 0.003	0.9047		
5	20 <sup>b</sup>	imine	q <sub>C</sub> (C=N) vs $\sigma$	-0.029 $\pm$ 0.003	0.9599	1	
6	20 <sup>b</sup>		q <sub>C</sub> (C=N) vs $\sigma^+$	-0.021 $\pm$ 0.003	0.9439	1	
7	20 <sup>b</sup>		q <sub>N</sub> (C=N) vs $\sigma$	0.029 $\pm$ 0.003	0.9569		
8	20 <sup>b</sup>		q <sub>N</sub> (C=N) vs $\sigma^+$	0.021 $\pm$ 0.003	0.9319		
9	12	imine	q <sub>C</sub> (C=N) vs $\sigma$	-0.026 $\pm$ 0.003	0.9357		
10	12		q <sub>C</sub> (C=N) vs $\sigma^+$	-0.016 $\pm$ 0.003	0.8880		
11	12		q <sub>N</sub> (C=N) vs $\sigma$	0.024 $\pm$ 0.003	0.9358		
12	12		q <sub>N</sub> (C=N) vs $\sigma^+$	0.015 $\pm$ 0.003	0.8880		
13	12	<i>N,N</i> -dialkylhydrazone	$\delta_N(\text{C=N})$ vs $\sigma$	19.6 $\pm$ 0.7	0.9945		
14	12		$\delta_N(\text{C=N})$ vs $\sigma^+$	12.5 $\pm$ 0.7	0.9865		
15	7		q <sub>C</sub> (C=N) vs $\sigma$	-0.044 $\pm$ 0.005	0.9588		
16	7		q <sub>C</sub> (C=N) vs $\sigma^+$	-0.024 $\pm$ 0.004	0.8674		
17	7 <sup>c</sup>	<i>N,N</i> -dialkylhydrazone	q <sub>C</sub> (C=N) vs $\sigma^+$	-0.019 $\pm$ 0.003	0.9040		
18	7		q <sub>N</sub> (C=N) vs $\sigma$	0.030 $\pm$ 0.005	0.9024		
19	7		q <sub>N</sub> (C=N) vs $\sigma^+$	0.019 $\pm$ 0.004	0.8572		
20	7 <sup>d</sup>		q <sub>N</sub> (N2) vs $\sigma$	0.011 $\pm$ 0.003	0.8624		
21	7 <sup>d</sup>	<i>N,N</i> -dialkylhydrazone	q <sub>N</sub> (N2) vs $\sigma^+$	0.007 $\pm$ 0.003	0.7640		
22	7		$\delta_N(\text{C=N})$ vs $\sigma$	11.7 $\pm$ 0.8	0.9869		
23	7		$\delta_N(\text{C=N})$ vs $\sigma^+$	7.3 $\pm$ 0.9	0.9562		
24	7		$\delta_N(\text{N2})$ vs $\sigma$	9.4 $\pm$ 1.5	0.9349		
25	7	<i>N</i> -benzoylhydrazone	$\delta_N(\text{N2})$ vs $\sigma^+$	5.6 $\pm$ 1.3	0.8655		
26	10		q <sub>C</sub> (C=N) vs $\sigma$	-0.032 $\pm$ 0.005	0.9257		
27	10		q <sub>C</sub> (C=N) vs $\sigma^+$	-0.019 $\pm$ 0.004	0.8751		
28	10 <sup>c</sup>		q <sub>C</sub> (C=N) vs $\sigma^+$	-0.016 $\pm$ 0.003	0.9086		
29	10	<i>N</i> -benzoylhydrazone	q <sub>N</sub> (C=N) vs $\sigma$	0.023 $\pm$ 0.002	0.9657		
30	10		q <sub>N</sub> (C=N) vs $\sigma^+$	0.015 $\pm$ 0.002	0.9336		
31	10		q <sub>N</sub> (N2) vs $\sigma$	-(9 $\pm$ 7) $\times 10^{-4}$	0.4650		
32	10		q <sub>N</sub> (N2) vs $\sigma^+$	-(9 $\pm$ 5) $\times 10^{-4}$	0.5884		
33	10	<i>N</i> -benzoylhydrazone	$\delta_N(\text{C=N})$ vs $\sigma$	14.6 $\pm$ 0.6	0.9924		
34	10		$\delta_N(\text{C=N})$ vs $\sigma^+$	9.2 $\pm$ 0.7	0.9751		
35	10		$\delta_N(\text{N2})$ vs $\sigma$	2.3 $\pm$ 0.3	0.9430		
36	10		$\delta_N(\text{N2})$ vs $\sigma^+$	1.4 $\pm$ 0.3	0.8873		
37	13 <sup>b</sup>	<i>N</i> -phenylhydrazone	q <sub>C</sub> (C=N) vs $\sigma$	-0.046 $\pm$ 0.005	0.9605		
38	13 <sup>b</sup>		q <sub>C</sub> (C=N) vs $\sigma^+$	-0.033 $\pm$ 0.004	0.9421		
39	13		q <sub>N</sub> (C=N) vs $\sigma$	0.023 $\pm$ 0.005	0.8645		
40	13		q <sub>N</sub> (C=N) vs $\sigma^+$	0.014 $\pm$ 0.004	0.8014		
41	13	<i>N</i> -phenylhydrazone	q <sub>N</sub> (N2) vs $\sigma$	0.009 $\pm$ 0.002	0.8657		
42	13		q <sub>N</sub> (N2) vs $\sigma^+$	0.005 $\pm$ 0.001	0.7874		
43	13 <sup>e</sup>		$\delta_N(\text{C=N})$ vs $\sigma$	14.6 $\pm$ 1.5	0.9846		
44	13 <sup>e</sup>		$\delta_N(\text{C=N})$ vs $\sigma^+$	10.5 $\pm$ 1.1	0.9835		
45	13 <sup>e</sup>	<i>N</i> -phenylhydrazone	$\delta_N(\text{N2})$ vs $\sigma$	8.0 $\pm$ 0.8	0.9855		
46	13 <sup>e</sup>		$\delta_N(\text{N2})$ vs $\sigma^+$	5.6 $\pm$ 1.1	0.9451		
47	14 <sup>b</sup>		hydrazone	q <sub>C</sub> (C=N) vs $\sigma$	-0.043 $\pm$ 0.005	0.9597	
48	14			q <sub>C</sub> (C=N) vs $\sigma^+$	-0.030 $\pm$ 0.004	0.9352	
49	14	q <sub>N</sub> (C=N) vs $\sigma$		0.026 $\pm$ 0.004	0.9334		
50	14	q <sub>N</sub> (C=N) vs $\sigma^+$		0.016 $\pm$ 0.003	0.8835		
51	14	hydrazone	q <sub>N</sub> (N2) vs $\sigma$	0.013 $\pm$ 0.002	0.9163		
52	14		q <sub>N</sub> (N2) vs $\sigma^+$	0.008 $\pm$ 0.002	0.8517		

<sup>a</sup>  $s$ , standard deviation;  $r$ , correlation coefficient. <sup>b</sup> *p*-NMe<sub>2</sub> excluded. <sup>c</sup> *p*-NO<sub>2</sub> excluded. <sup>d</sup> *p*-NMe<sub>2</sub>, *p*-Me, and *p*-CN excluded. <sup>e</sup> In DMSO with *p*-OMe, *p*-Me, H, *p*-Cl, and *p*-NO<sub>2</sub> substituents;  $\delta_N$  values were taken from ref 12.

ca. 15 (line 43) for the C=N nitrogen and ca. 8 for N2 (line 45), which we calculated with the values for the phenylhydrazones (**13**) in DMSO,<sup>12</sup> are close to our hydrazone values, with the exception of N2 in **10**. The resonance of the C=N nitrogen of the hydrazones seems to be less sensitive to phenyl substitution than that of the C=N nitrogen of the imines. The N2 resonance also shows a response to the substituent, but to a lesser extent. The good or at least satisfactory fits and positive slopes for all these correlations, together with the q<sub>N</sub> vs  $\sigma$  correlations discussed above, indicate that the  $\delta_N$  variations accompanying substitution are electronic in origin and that the higher the electron density on the

nitrogen, the lower the frequency of nitrogen resonance (at a higher field; more negative  $\delta_N$  values). This represents normal behavior.

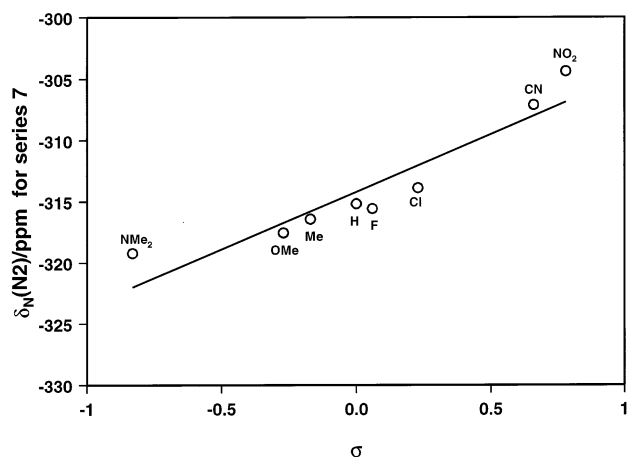
**Cross-Correlations.** A more explicit view of the polarization character of the C=N/C=N-N units of the imines and hydrazones is provided by the different correlations and cross-correlations of the q<sub>C</sub>(C=N), q<sub>N</sub>(C=N), q<sub>N</sub>(N2),  $\delta_C$ , and  $\delta_N$  values. The slopes of the linear q<sub>N</sub>(C=N) vs q<sub>C</sub>(C=N) plots for series **7**, **10**, **13**, and **14** are -0.79 (Table 3, line 14; Figure 3), -0.70 (line 20), -0.74 (line 26), and -0.77 (line 30), respectively. The slopes for the q<sub>N</sub>(N2) vs q<sub>C</sub>(C=N) plots for series **7**, **13**, and **14** are -0.29 (Table 3, line 15; Fig. S3), -0.27 (line



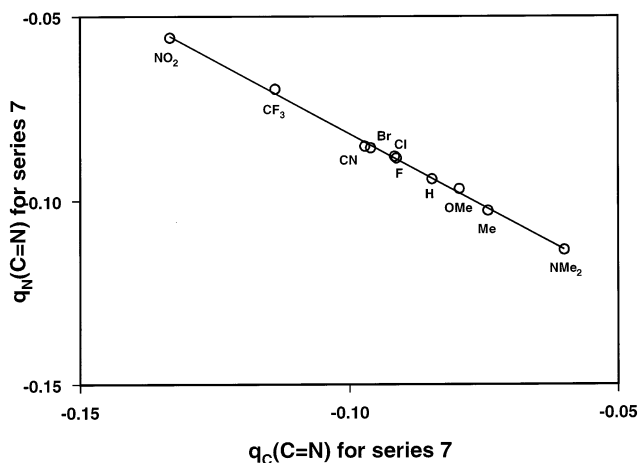
**TABLE 3.** Statistical Data for Different Correlations and Cross-Correlations of  $^{13}\text{C}$  and  $^{15}\text{N}$  NMR Chemical Shifts and Atomic Charges of the C=N Carbon, C=N Nitrogen, or N2 for Imine Series 12, 15, and 20 and for Hydrazone Series 7, 10, 13, and 14<sup>a</sup>

line	series	type of compound	correlation	slope $\pm s$	$r$	ref
1	15	imine	$\delta_{\text{C}}(\text{C}=\text{N})$ vs $q_{\text{C}}(\text{C}=\text{N})$	$52 \pm 14$	0.8192	1
2	15		$q_{\text{N}}(\text{C}=\text{N})$ vs $q_{\text{C}}(\text{C}=\text{N})$	$-1.06 \pm 0.02$	0.9990	1
3	20	imine	$q_{\text{N}}(\text{C}=\text{N})$ vs $q_{\text{C}}(\text{C}=\text{N})$	$-1.00 \pm 0.02$	0.9989	1
4	12	imine	$\delta_{\text{C}}(\text{C}=\text{N})$ vs $q_{\text{C}}(\text{C}=\text{N})$	$69 \pm 14$	0.8716	
5	12		$\delta_{\text{N}}(\text{C}=\text{N})^b$ vs $q_{\text{N}}(\text{C}=\text{N})$	$550 \pm 40$	0.9830	
6	12		$\delta_{\text{N}}(\text{C}=\text{N})$ vs $\delta_{\text{C}}(\text{C}=\text{N})$	$-6 \pm 2$	0.8357	
7	12		$q_{\text{N}}(\text{C}=\text{N})$ vs $q_{\text{C}}(\text{C}=\text{N})$	$-0.94 \pm 0.01$	0.9992	
8	7	<i>N,N</i> -dialkylhydrazone	$\delta_{\text{C}}(\text{C}=\text{N})$ vs $q_{\text{C}}(\text{C}=\text{N})^c$	$95 \pm 9$	0.9808	
9	7		$\delta_{\text{N}}(\text{C}=\text{N})$ vs $q_{\text{N}}(\text{C}=\text{N})$	$325 \pm 66$	0.8956	
10	7		$\delta_{\text{N}}(\text{N}2)$ vs $q_{\text{N}}(\text{N}2)^d$	$170 \pm 102$	0.6416	
11	7		$\delta_{\text{N}}(\text{C}=\text{N})$ vs $\delta_{\text{C}}(\text{C}=\text{N})$	$-2.4 \pm 0.3$	0.9700	
12	7		$\delta_{\text{N}}(\text{N}2)$ vs $\delta_{\text{C}}(\text{C}=\text{N})$	$-2.1 \pm 0.2$	0.9622	
13	7		$\delta_{\text{N}}(\text{C}=\text{N})$ vs $\delta_{\text{N}}(\text{N}2)$	$1.14 \pm 0.11$	0.9740	
14	7		$q_{\text{N}}(\text{C}=\text{N})$ vs $q_{\text{C}}(\text{C}=\text{N})$	$-0.79 \pm 0.01$	0.9988	
15	7		$q_{\text{N}}(\text{N}2)$ vs $q_{\text{C}}(\text{C}=\text{N})^e$	$-0.29 \pm 0.05$	0.9324	
16	7		$q_{\text{N}}(\text{N}2)$ vs $q_{\text{N}}(\text{C}=\text{N})^e$	$0.37 \pm 0.06$	0.9298	
17	10	<i>N</i> -benzoylhydrazone	$\delta_{\text{C}}(\text{C}=\text{N})$ vs $q_{\text{C}}(\text{C}=\text{N})$	$82 \pm 13$	0.9281	
18	10		$\delta_{\text{N}}(\text{C}=\text{N})$ vs $q_{\text{N}}(\text{C}=\text{N})$	$591 \pm 54$	0.9682	
19	10		$\delta_{\text{N}}(\text{N}2)$ vs $q_{\text{N}}(\text{N}2)$	$-284 \pm 89$	0.7930	
20	10		$q_{\text{N}}(\text{C}=\text{N})$ vs $q_{\text{C}}(\text{C}=\text{N})$	$-0.70 \pm 0.04$	0.9873	
21	10		$q_{\text{N}}(\text{N}2)$ vs $q_{\text{C}}(\text{C}=\text{N})$	$0.011 \pm 0.018$	0.2387	
22	10		$q_{\text{N}}(\text{N}2)$ vs $q_{\text{N}}(\text{C}=\text{N})$	$-0.02 \pm 0.027$	0.2730	
23	13	<i>N</i> -phenylhydrazone	$\delta_{\text{C}}(\text{C}=\text{N})^f$ vs $q_{\text{C}}(\text{C}=\text{N})$	$76 \pm 17$	0.9132	
24	13		$\delta_{\text{N}}(\text{C}=\text{N})^g$ vs $q_{\text{N}}(\text{C}=\text{N})$	$370 \pm 40$	0.9903	
25	13		$\delta_{\text{N}}(\text{N}2)^g$ vs $q_{\text{N}}(\text{N}2)$	$550 \pm 40$	0.9919	
26	13		$q_{\text{N}}(\text{C}=\text{N})$ vs $q_{\text{C}}(\text{C}=\text{N})$	$-0.74 \pm 0.01$	0.9997	
27	13		$q_{\text{N}}(\text{N}2)$ vs $q_{\text{C}}(\text{C}=\text{N})$	$-0.27 \pm 0.01$	0.9920	
28	13		$q_{\text{N}}(\text{N}2)$ vs $q_{\text{N}}(\text{C}=\text{N})$	$0.36 \pm 0.02$	0.9899	
29	14	hydrazone	$\delta_{\text{C}}(\text{C}=\text{N})^f$ vs $q_{\text{C}}(\text{C}=\text{N})$	$99 \pm 16$	0.9631	
30	14		$q_{\text{N}}(\text{C}=\text{N})$ vs $q_{\text{C}}(\text{C}=\text{N})$	$-0.772 \pm 0.004$	0.9999	
31	14		$q_{\text{N}}(\text{N}2)$ vs $q_{\text{C}}(\text{C}=\text{N})$	$-0.38 \pm 0.01$	0.9952	
32	14		$q_{\text{N}}(\text{N}2)$ vs $q_{\text{N}}(\text{C}=\text{N})$	$0.49 \pm 0.02$	0.9958	

<sup>a</sup>  $s$ , standard deviation;  $r$ , correlation coefficient. <sup>b</sup> *p*-CN and *p*-NMe<sub>2</sub> excluded. <sup>c</sup> *p*-CN excluded. <sup>d</sup> *p*-NO<sub>2</sub> and *p*-CN excluded. <sup>e</sup> *p*-CH<sub>3</sub> and *p*-CN excluded. <sup>f</sup>  $\delta_{\text{C}}$  values were taken from ref 9. <sup>g</sup>  $\delta_{\text{N}}$  values were taken from ref 12.

**FIGURE 2.** Plot of the  $^{15}\text{N}$  NMR chemical shifts of N2 for series 7 in  $\text{CDCl}_3$  vs Hammett substituent constants  $\sigma$ .

27), and  $-0.38$  (line 31), respectively, whereas the slope is 0.011 only for series 10 (line 21). In accordance with the behavior of the imines, the atomic charges on the C=N carbon and the C=N nitrogen of the hydrazones display an inverse trend. However, in contrast with the behavior of the imines, for which  $\Delta q_{\text{N}}(\text{C}=\text{N})/\Delta q_{\text{C}}(\text{C}=\text{N})$  is shown to be close to  $-1.0$  (Table 3; lines 2, 3, and 7), for the hydrazones, the charge on the C=N nitrogen is less sensitive to substitution than that on the C=N carbon. The counterpart of the variable charge on the

**FIGURE 3.** Cross-correlation between the atomic charge of the C=N nitrogen and that of the C=N carbon for series 7.

carbon seems to be distributed on both nitrogen atoms. In addition to the difference in the slopes of the  $q_{\text{N}}(\text{C}=\text{N})$  vs  $q_{\text{C}}(\text{C}=\text{N})$  plots between the imines and hydrazones, a marked difference is to be seen between *N,N*-dialkylhydrazones (7) and *N*-alkyl-*N*-benzoylhydrazones (10) when the dependence of the charges of the C=N nitrogen and N2 on the phenyl substituent is compared. For series 7, the  $q_{\text{N}}(\text{C}=\text{N})$  and  $q_{\text{N}}(\text{N}2)$  display a similar trend, although N2 exhibits a diminished change, only about 40% of that observed for the C=N (Table 3; lines 14–16). For series

**10**, the charge on N2 hardly varies with the substituent (Table 3; lines 20–22). This agrees with the different behavior of the  $^{15}\text{N}$  NMR shifts of N2 for series **7** and **10** discussed above (Table 2; cf. lines 24 and 35). In summary, while the polarizable unit in the imines is the C=N fragment, in the hydrazones, the charge at the other end of the dipole seems to be distributed on both nitrogen atoms. The hydrazide character of benzoylhydrazones is clearly indicated by the insensitivity of both the charge and  $\delta_{\text{N}}$  of N2 to phenyl substitution. Obviously, the amide resonance prevents interaction of the lone pair of N2 with the C=N unit.

For the hydrazones, the dependence of the C=N carbon  $^{13}\text{C}$  NMR chemical shift on the charge on the carbon is significant. The slopes of the plots  $\delta_{\text{C}}(\text{C}=\text{N})$  vs  $q_{\text{C}}(\text{C}=\text{N})$  are 95 and 82 ppm/electron, respectively, for series **7** and **10** (Table 3; lines 8 and 17; cf. Figure S4) and **17**. For the hydrazones **14**, the slope is 99 ppm/electron, and for the *N*-phenylhydrazones **13**, the slope is 76 ppm/electron (lines 29 and 23, respectively). In all cases, deshielding (increased shift) of the carbon is observed with decreasing electron density (less negative atomic charge) on the carbon. The C=N carbon chemical shift of the hydrazones seems to be clearly more sensitive to the atomic charge on the carbon than that for the imines. For the imine series **15** and **12**, the slopes of the plots  $\delta_{\text{C}}(\text{C}=\text{N})$  vs  $q_{\text{C}}(\text{C}=\text{N})$  are only 52 and 69 ppm/electron, respectively (Table 3; lines 1 and 4).<sup>1a</sup>

For the imine series **12**, a slope of 550 ppm/electron is observed for the plot of  $\delta_{\text{N}}(\text{C}=\text{N})$  vs  $q_{\text{N}}(\text{C}=\text{N})$  (Table 3; line 5). For the *N,N*-dialkylhydrazones **7**, the dependences of the C=N nitrogen and N2 resonances on the electron density on the nitrogen in question are different. Correlation coefficients of 325 and 170 ppm/electron, respectively, are observed (lines 9 and 10). For series **10**, the slope of the plot  $\delta_{\text{N}}(\text{C}=\text{N})$  vs  $q_{\text{N}}(\text{C}=\text{N})$  is 590 ppm/electron (Table 3; line 18), and that for series **13** is 370 ppm/electron (line 24). The former value is close to that observed for series **12**, and the latter value is very similar to that observed for series **7**. As regards the plot of  $\delta_{\text{N}}(\text{N}2)$  vs  $q_{\text{N}}(\text{N}2)$ , the slopes are  $-284$  and  $550$  ppm/electron, respectively, for series **10** and **13** (Table 3; lines 19 and 25, respectively). Both of these values differ considerably from the slope of  $170$  ppm/electron observed for series **7**. For series **13**, the correlations in question are very good for both C=N and N2, while for series **10**, the correlation is satisfactory for C=N and poor for N2. For series **7**, both correlations are poor. With the exception of  $\delta_{\text{N}}(\text{N}2)$  for series **10**, in all cases, the less negative the electron density of the atom, the lower the field of nitrogen resonance. This is according to the generalized electronic effect.

The C=N carbons of the hydrazones carry significantly more negative atomic charges from  $-0.13$  to  $-0.06$  (cf. Tables S1, S4, S5, and S6) than those previously observed for the C=N carbon of the imines (from  $-0.06$  to  $-0.003$ )<sup>1a</sup> or now observed for the imine series **12** (Table S2, from  $-0.06$  to  $-0.02$ ). This is consistent with the  $^{13}\text{C}$  NMR chemical shift data, which show that the C=N carbon of the hydrazones resonates at a lower frequency (i.e., with reduced shift values) than that of the imines (cf. Table 1). This difference suggests a more significant contribution of the resonance form **4** (cf. Scheme 1) in the case of the imines than in the case of the hydrazones.

Also, the C=N nitrogens of the hydrazones (**7**, **13**, and **14**) both possess more negative charges and resonate at a lower frequency than those of the imines (**12**). The hydrazones belonging in series **10**, however, behave analogously to the imines in series **12**.

In light of the present theoretical calculations and the correlations observed, the higher dependence of the C=N carbon  $^{13}\text{C}$  NMR chemical shift of the hydrazones on the phenyl substituent as compared with the imines (cf. Table 1) can be ascribed primarily to two main reasons: (i) the higher sensitivity of the chemical shift at the probe site to changes in electron density, i.e., a higher shift:charge ratio, and (ii) the higher sensitivity of the charge on the carbon to substitution. Of these two reasons, the former seems to be the more important. Both of these facts indicate that the charge distribution on the C=N unit is different for hydrazones and imines. For imines, we recently suggested a significant contribution of the substituent-sensitive inherent polarization of the C=N unit, the main contributing structures being **3** and **4** (Scheme 1).<sup>1a</sup> As has already been discussed, for imines, the  $\rho_{\text{R}}$  values are negative but small. This indicates a low significance of structure **5** and structure **6**, too.

**Differences in the Mechanism of Polarization of the C=N Unit of Imines and Hydrazones.** Scrutiny of the information derived from the  $^{13}\text{C}$  and  $^{15}\text{N}$  NMR chemical shifts and the PM3 atomic charges reveals several characteristic differences between the imines and hydrazones.

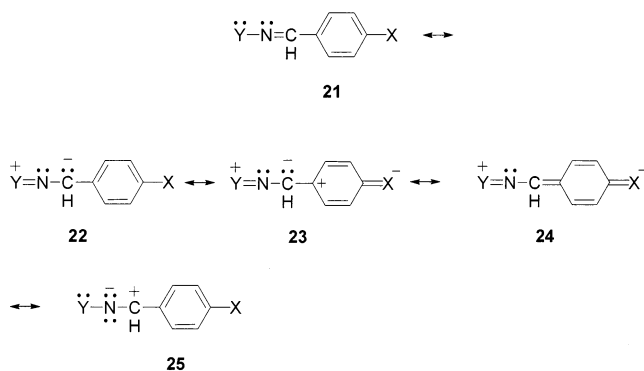
(i) On average, the  $\rho_{\text{I}}$  or  $\rho_{\text{F}}$  values derived from DSP analysis of the  $^{13}\text{C}$  NMR chemical shifts are somewhat larger for the hydrazones. (ii) For the  $\rho_{\text{R}}$  values, a considerable difference is seen (5–10 times larger for the hydrazones as compared with those for the imines). (iii) For the hydrazones, both the carbon and nitrogen of the C=N unit are shielded as compared with imines. (iv) The atomic charges on the C=N unit are more negative and more sensitive to effects of substituents for the hydrazones. (v) The mutual atomic charge behavior for the C=N carbon and nitrogen also differs. For the imines, the slope of the plot of  $q_{\text{N}}(\text{C}=\text{N})$  vs  $q_{\text{C}}(\text{C}=\text{N})$  is negative and close to  $-1$ , whereas, as an example, it is  $-0.79$  for the hydrazone series **7**. For the plot of  $q_{\text{N}}(\text{N}2)$  vs  $q_{\text{C}}(\text{C}=\text{N})$ , the slope is only  $-0.29$ . Clearly, for the hydrazones, the charge is distributed on both nitrogen atoms. The facts listed above suggest a difference between the imines and hydrazones in terms of the mechanism by which the substituents induce changes in the charges and the NMR chemical shifts of the nuclei of the C=N group. The behavior of the benzoylhydrazones seems to be intermediate between those of the imines and the other hydrazones. For the imines, the substituent dependence of the  $^{13}\text{C}$  and  $^{15}\text{N}$  NMR chemical shifts on the benzyldenic substituent X can largely be explained by comparison of the contributions of the resonance forms **3–6** in Scheme 1.<sup>1a</sup> To date, no explicit explanation has been given for the behavior of the hydrazones. However, resonance structure **22** was proposed by Gordon et al. (cf. Scheme 2).<sup>9</sup> The basic question is that of whether the effect of Y is conjugative (if there is a lone pair in use, as has been proposed), inductive, or steric.

For a better understanding of the behavior of the hydrazones vs that of the imines, we compared the  $\rho_{\text{F}}(\text{X})$  and  $\rho_{\text{R}}(\text{X})$  values of the compounds studied in this work

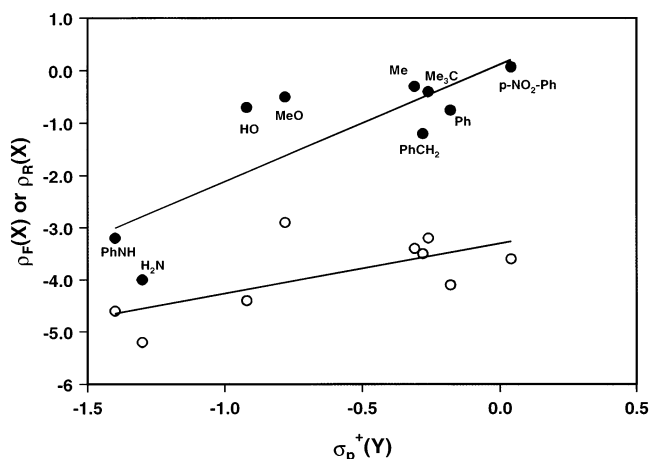
**TABLE 4.** Effect of Substituent Y in Y-N=CH-C<sub>6</sub>H<sub>4</sub>-p-X System on  $\rho_R$  and  $\rho_F$  Values Describing the Dependence of <sup>13</sup>C NMR Chemical Shifts of the C=N Carbon on the Benzylidenic Substituent X<sup>a,b</sup>

Y	$\sigma_p^+$	$\delta_C(\text{C=N})$	$q_C(\text{C=N})$	$\rho_F$	$\rho_R$	C=N bond order (bond length)	=N-Y bond order (bond length)	=C-C(Ph) bond order (bond length)	ref <sup>c</sup>
NH <sub>2</sub>	-1.30	142.77	-0.0795	-5.2	-4.0	1.8541 (1.3020)	1.0697 (1.3824)	1.0190 (1.4652)	9
NHPh	-1.40	137.25	-0.0771	-4.6	-3.2	1.8564 (1.3013)	1.0473 (1.3914)	1.0186 (1.4653)	9
HO	-0.92	150.33	-0.0531	-4.4	-0.7	1.8961 (1.2982)	1.0130 (1.4007)	1.0158 (1.4660)	9, 15
MeO	-0.78	148.26	-0.0489	-2.9	-1.2	1.9064 (1.2958)	0.9810 (1.4264)	1.0130 (1.4668)	13
Me	-0.31	162.44	-0.0452	-3.4	-0.30	1.9161 (1.2919)	1.0130 (1.4499)	1.0090 (1.4682)	13
(CH <sub>3</sub> ) <sub>3</sub> C	-0.26	155.08	-0.0295	-3.2	-0.4	1.9285 (1.2883)	0.9720 (1.4838)	1.0041 (1.4704)	13
Ph	-0.18	160.34	-0.0289	-4.1	-0.75	1.8891 (1.2939)	1.0330 (1.4310)	1.0113 (1.4676)	this work
PhCH <sub>2</sub>	-0.28	161.93	-0.0340	-3.5	-0.5	1.9217 (1.2910)	0.9892 (1.4656)	1.0077 (1.4686)	10
p-NO <sub>2</sub> -C <sub>6</sub> H <sub>4</sub>	+0.04	162.46	0.0042	-3.6	0.07	1.8852 (1.2939)	1.04570 (1.4264)	1.0145 (1.4666)	14

<sup>a</sup>  $\delta_C(\text{C=N})$  and  $q_C(\text{C=N})$  values and C=N, =N-Y, and =C-C(Ph) bond orders and bond lengths (Å) are given for substitution X = H. =C-C(Ph) refers to the bond between the C=N carbon and the substituted phenyl ring. <sup>b</sup>  $\rho$  values were calculated in this work via eq 1:  $\text{SCS} = \rho_F \sigma_F + \rho_R \sigma_R$ , with the aid of the literature <sup>13</sup>C NMR data, with the exception of Y = Ph (series **12**), for which the NMR data were determined in this work. <sup>c</sup> Reference for the <sup>13</sup>C NMR chemical shift data used to calculate the  $\rho_F$  and  $\rho_R$  values.

**SCHEME 2**

with the corresponding values that we derived from the literature NMR shift data (Y-N=CH-C<sub>6</sub>H<sub>4</sub>-p-X; Table 4). The correlation parameters  $\rho_F(X)$  and  $\rho_R(X)$  for series **12** (Y = -Ph) are based on <sup>13</sup>C NMR shifts recorded in this study. For the other series, i.e., Y = -Me, -CMe<sub>3</sub>, -CH<sub>2</sub>Ph, -C<sub>6</sub>H<sub>4</sub>-p-NO<sub>2</sub>, -OMe, -OH, -NH<sub>2</sub> (series **13**), and -NHPh (series **14**), we calculated  $\rho_F(X)$  and  $\rho_R(X)$  with the aid of <sup>13</sup>C NMR shift data from the literature. The fact that the *sensitivity* of the electronic character of the C=N function to *electron donation/electron withdrawal by the phenyl substituent X* is adjusted by the electronic effects of Y is seen on inspection of Figure 4. Both the  $\rho_F(X)$  and  $\rho_R(X)$  values from Table 4 can be successfully correlated with the  $\sigma_p^+$  values of group Y,  $\sigma_p^+(Y)$ . Thus, the effect of Y is electronic in nature. We also examined correlations with  $\sigma$ ,  $\sigma_I$ , and R, but these were less successful, indicating that both inductive and resonance effects contribute. The varying sources of the NMR data (different sample concentrations, varying set of substitutions) account for the fact that the goodness of the correlation is not very high. Figure 4 can be rationalized by inspecting the contributions of the different resonance forms in Schemes 1 and 2. For imines, when Y is an electron-withdrawing group or can at least

**FIGURE 4.** Plots of the correlation parameters  $\rho_F(X)$  (○) and  $\rho_R(X)$  (●) (determined with respect to phenyl substituent X) vs substituent constant  $\sigma_p^+(Y)$  with varying Y for Y-N=CH-C<sub>6</sub>H<sub>4</sub>-p-X.

stabilize **4** (-Me, -CMe<sub>3</sub>, -Ph, -CH<sub>2</sub>Ph, -C<sub>6</sub>H<sub>4</sub>-p-NO<sub>2</sub>), the contribution of **4** (Scheme 1) will increase as a function of  $\sigma_p^+(Y)$ . With electron-donating substituents X, its contribution further increases. This will result in a more positively charged C=N carbon (deshielding) and negative  $\rho_F$  and  $\rho_R$  (the latter via structure **5**) values. On the other hand, although Y is inductively electron withdrawing but at the same time electron donating via resonance (-NH<sub>2</sub>, -NHPh, -OH, or -OMe), resonance structure **22** (Scheme 2) is stabilized. As regards the effect of substituent X, electron-withdrawing substituents stabilize **22** inductively and make possible the contribution of **23** through resonance. As a consequence, the C=N carbon exhibits more negative charges. This results in negative  $\rho_F$  and  $\rho_R$  (the latter via structure **23**) values.

Figure 4 clearly shows that the hydrazones exhibit characteristics that are common for all compounds possessing an atom with a lone pair attached to the C=N

nitrogen, i.e., when Y is a group capable of conjugative electron donation. The correlations in Figure 4 can be explained by different balances between the possible resonance structures for the imines (Scheme 1) and the hydrazones and related compounds (Scheme 2). The substituents Y capable of electron donation by resonance ( $Y = -NH_2, -NHPh, -OMe, -OH$ ; group **A**) result in more negative  $\rho_R(X)$  values the more negative  $\sigma_p^+(Y)$  is, indicating an increase in the contribution of **22** (Scheme 2). The fact that the  $\rho_R(X)$  values are highly negative for group **A** means that the resonance effects of the substituents X must be resonance-induced polar effects (**22**  $\leftrightarrow$  **23**) and not the normal resonance effects (**22**  $\leftrightarrow$  **24**). The latter case would lead to  $\rho_R(X) > 0$ .

It seems evident that the resonance-induced polar effects (**5**, Scheme 1) are not of high importance (only small negative  $\rho_R$ ) for the imines ( $Y = -Me, -CMe_3 -Ph, -CH_2Ph, -C_6H_4-p-NO_2$ ; group **B**). The other possibility is that in both cases, i.e., for the compounds in groups **A** and **B**, both the normal resonance effect [**6** in Scheme 1, **24** in Scheme 2; leading to  $\rho_R(X) > 0$ ] and the inverse resonance-induced polar effect [**5** in Scheme 1, **23** in Scheme 2; leading to  $\rho_R(X) < 0$ ] operate; however, in the case of the imines (group **B**), the two effects compensate each other, while in the case of group **A**, the inverse effect is overwhelming.

For the imines (group **B**), the  $\rho_F$  values are clearly negative in all cases, varying within only a narrow range. Obviously, the contribution of **4** does not vary largely with the different Ys studied. Electron-withdrawing phenyl substituents X inductively destabilize **4**, and a decrease in the imine carbon charge (a less positive charge), a shielding effect, and  $\rho_F(X) < 0$  result. For the hydrazones and related compounds (group **A**), an increased electron donation by Y [a more negative  $\sigma_p^+(Y)$ ] stabilizes **22**. Consequently, its contribution increases, leading to a higher sensitivity of the electronic character of the C=N function to phenyl substitution via the inductive effects of X. Electron-withdrawing substituents X inductively stabilize structure **22**, and a decrease in the charge on the imine carbon (more negative charges), a shielding effect, and  $\rho_F(X) < 0$  result. The varying sensitivity to X is seen as a dependence of  $\rho_F(X)$  on  $\sigma_p^+(Y)$  with a positive slope.

Additional support is lent to our conclusions by an inspection of the plot in Figure 5, where  $\rho_R(X)$  is plotted against  $\delta_C(C=N)$  for the unsubstituted derivatives, i.e., X = H, for the series with different Ys. The more shielded the carbon, the more sensitive its  $^{13}C$  NMR shift is to conjugative effects by X. We consider the shielding of the C=N carbon to reflect the fact that the contribution of resonance structure **22** is increased. This conclusion could be verified by the plots shown in Figures 6 and 7. In Figure 6, it is clearly seen that shielding corresponds to the increase in electron density at the C=N carbon. Figure 7 shows correlation between  $\rho_R$  and  $\rho_F$  values and  $q_C(C=N)$ . Both parameters turn more negative when the atomic charge at the C=N carbon becomes more negative. According to our interpretation, the inductive effects of substituents X affect the stabilities of forms **4** and **22** with practically the same efficiency, while the resonance effects overwhelmingly affect via the interaction **22**  $\leftrightarrow$  **23**. Thus, it can be concluded that particularly the sensitivity of the  $^{13}C$  chemical shift of the C=N carbon

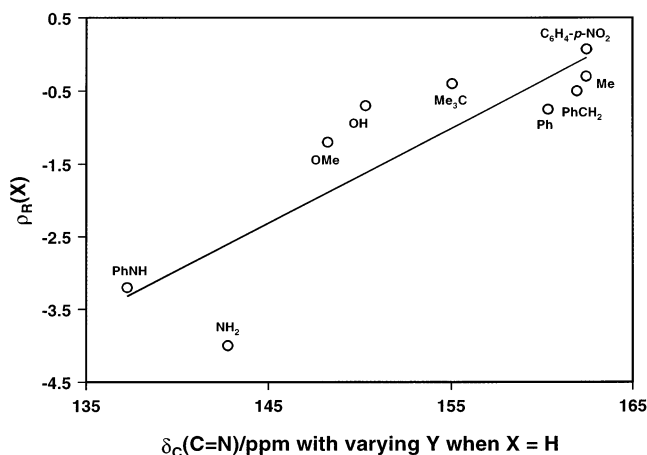


**FIGURE 5.** Plot of the correlation parameter  $\rho_R(X)$  (determined with respect to phenyl substituent X) vs the C=N carbon  $^{13}C$  NMR chemical shift for the phenyl unsubstituted derivative  $Y-N=CH-C_6H_5$  with varying Y.

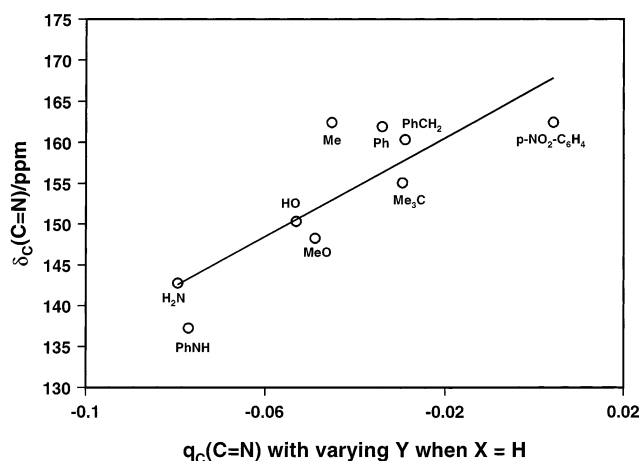


**FIGURE 6.** Plot of the C=N carbon  $^{13}C$  NMR chemical shift in  $CDCl_3$  for the phenyl unsubstituted derivative  $Y-N=CH-C_6H_5$  vs the atomic charge of the C=N carbon with varying Y.

to the electronic resonance effects of the phenyl substituent X, i.e.,  $\rho_R(X)$ , is a useful tool for evaluating the electrophilicity of the C=N carbon.

The bond order/bond length data in Table 4 further support the above conclusions. For compounds in group **A**, the C=N bond order is lower and the bond is lengthened, while the =N-Y and =C-C(Ph) bond orders are higher and the bonds are shortened as compared with compounds in group **B**. The imine derivatives possessing an aromatic ring attached directly to the C=N nitrogen ( $Y = Ph$  or  $p-NO_2-C_6H_4$ ) show bond orders between those typical for group **A** and those typical for other members of group **B**. Further, when varying Y, good or at least fair correlations with slopes of  $(6.2 \pm 0.7) \times 10^{-2}$  ( $r = 0.9650$ ) and  $1.54 \pm 0.10$  ( $r = 0.9895$ ), respectively, were observed between the C=N bond order and  $\sigma_p^+(Y)$  and between the C=N bond order and  $q_C(C=N)$  when  $Y = Ph$  and  $p-NO_2-C_6H_4$  were excluded.

The present results show that the sensitivity of the electronic character of the C=N function in  $Y-N=CH-C_6H_4-p-X$  to electron donation/electron withdrawal by the phenyl substituent X is adjusted by the electronic effects of Y. This is revealed by the behavior of the  $^{13}C$



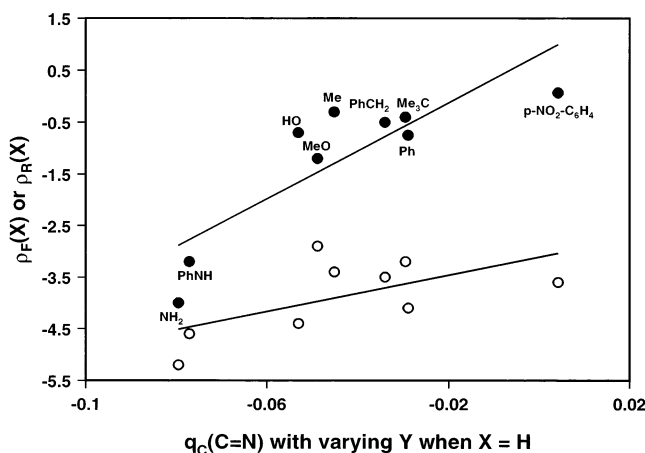


**FIGURE 7.** Plots of the correlation parameters  $\rho_F(X)$  (○) and  $\rho_R(X)$  (●) (determined with respect of phenyl substituent X) vs the atomic charge of the C=N carbon for  $Y=N-CH-C_6H_5$  with varying Y.

or  $^{15}N$  NMR chemical shifts. Related results have recently been obtained by Liu et al. in theoretical bond dissociation energy studies concerning *para*-substituted aromatic silanes<sup>17</sup> and *para*-substituted anilines.<sup>18</sup> For instance, for their 4- $Y-C_6H_4-Z-X$  system ( $Z = SiH_2$ ;  $X = H, F, Cl, \text{ or } Li$ ;  $Y = NO_2, CHO, CN, CF_3, COCH_3, CONH_2, COOH, F, Cl, H, Me, SMe, OMe$ ), they state that “the direction and magnitude of the effect of substituents Y have some important dependence on the polarity of the Z–X bond undergoing homolysis.”<sup>17</sup> Their results as well as ours indicate that there prevails an interesting interaction over the aromatic and side-chain systems. The item is under continuous interest.

## Conclusions

The extensive data relating to the azomethines, hydrazones, and related compounds derived from substituted benzaldehydes have shown that the substituent effects on the C=N  $^{13}C$  and/or C=N  $^{15}N$  NMR chemical shifts can be explained by considering the different resonance structures depicted in Schemes 1 and 2. For these compounds possessing a C=N double bond, the magnitude of the negative  $\rho_R$  derived from calculations involving the  $^{13}C$  NMR chemical shifts of the C=N carbon with respect to substituent X is a useful tool for evaluating the detailed electronic character of the C=N double bond. The strength of the effect of X varies characteristically as a function of substituent Y. In Figure 4, the  $\rho_R$  and  $\rho_F$  values observed with substituent X are plotted against the  $\sigma_p^+$  value of substituent Y. These plots illustrate a novel way of using the Hammett-type parameters. The justification of this treatment was verified

by  $\delta_C(C=N)$  vs  $q_C(C=N)$ ,  $\rho_F/\rho_R$  vs  $q_C(C=N)$ , the C=N bond order vs  $\sigma_p^+(Y)$ , and the C=N bond order vs  $q_C(C=N)$  correlations with varying Y. According to our interpretation, the inductive effects of substituent X affect the stabilities of forms **4/25** and **22** with practically the same efficiency, while the resonance interaction **22**  $\leftrightarrow$  **23** is more efficient than the interaction **4**  $\leftrightarrow$  **5**. We conclude that these results can be useful as concerns an explanation of the reactivities of the compounds in question toward nucleophilic agents; this property is governed by the electrophilicity of the C=N carbon.

## Experimental Section

**General Procedures.** Melting points are uncorrected. All new compounds (see Table S1) gave satisfactory microanalyses (C, H, N).

**Synthesis of Benzylidene Derivatives 12.** Aniline (2 mmol) and the appropriate aromatic aldehyde (2 mmol) were dissolved together in ethanol (10 mL) and left to stand overnight at room temperature. The solvent was evaporated off, and the products were recrystallized from ethanol or diisopropyl ether. The yields were 77–90%.

**NMR Measurements.** NMR spectra were recorded at 27 °C on an NMR spectrometer operating at 125.78 MHz for  $^{13}C$  and 50.688 MHz for  $^{15}N$  on 0.4 M solutions in  $CDCl_3$ .  $^{13}C$  NMR spectra were referenced internally to tetramethylsilane (0.00 ppm), while  $^{15}N$  NMR spectra were referenced externally to  $CH_3NO_2$  (0.00 ppm) containing 10% w/w  $CD_3NO_2$  for locking purposes. The signal of the deuterium of the solvent was used as a lock signal for  $^{13}C$  NMR spectra.  $^{13}C$  NMR spectra were acquired with  $^1H$  broad-band decoupling and NOE  $^1H$  nondecoupling techniques.  $^{13}C$  NMR spectra were acquired with the following conditions: spectral width = 30 kHz, 32 K data points ( $^1H$  decoupled)/64 K data points ( $^1H$  coupled), digital resolution = 0.92 Hz/point ( $^1H$  decoupled)/0.46 Hz/point ( $^1H$  coupled), pulse width = 4.35  $\mu s$  (45°), acquisition time = 1.09 s ( $^1H$  decoupled)/2.18 s ( $^1H$  coupled), number of transients = 1000–12000, pulse delay = 3 s ( $^1H$  decoupled)/5 s ( $^1H$  coupled), pulse sequence = (JEOL) SGBCM ( $^1H$  decoupled)/SGNOE ( $^1H$  coupled). Exponential windowing with a line-broadening term of 2 Hz ( $^1H$  decoupled)/1 Hz ( $^1H$  coupled) was applied prior to Fourier transformation.  $^{15}N$  NMR spectra were acquired with refocused INEPT technique optimized on 8 Hz.  $^{15}N$  NMR spectra were acquired with the following conditions: 90° flip angle, pulse recycle time = 5.1 s, spectral width = 25 kHz consisting of 64 K data points (digital resolution 0.39 Hz/point), pulse sequence = (JEOL) INPTR. Exponential windowing with a line-broadening term of 1 Hz was applied prior to Fourier transformation.

**Statistical Calculations.** The sources of the substituent constants are as follows:  $\sigma, \sigma^+$ , ref 11;  $\sigma_F, \sigma_R$ , ref 16, except  $\sigma_F$  and  $\sigma_R$  for Br, ref 11.

**PM3 Calculations.** Three-dimensional structures of the compounds were composed by using the program SYBYL,<sup>19</sup> and the structures thus obtained were optimized with the Tripos force field. The resulting conformations were used as starting structures for the semiempirical calculations of conformations, heats of formation, and atomic charges. These calculations were performed by using the semiempirical quantum mechanical method PM3<sup>20</sup> of the program MOPAC 7.0.<sup>21</sup> All structures were optimized without any restriction. The quantum chemical calculations were processed on the SGI “Octane” (2  $\times$  R 12 000) computer of the University of Potsdam.

(13) Jennings, W. B.; Wilson, V. E.; Boyd, D. R.; Couter, P. B. *Org. Magn. Reson.* **1983**, *21*, 279.

(14) Akaba, R.; Sakuragi, H.; Tokumaru, K. *Bull. Chem. Soc. Jpn.* **1985**, *58*, 1186.

(15) Danoff, A.; Franzen-Sieveling, M.; Lichter, R. L.; Fanso-Free, S. N. *Y. Org. Magn. Reson.* **1979**, *12*, 83.

(16) Taft, R. W.; Topsom, R. D. *Prog. Phys. Org. Chem.* **1987**, *16*, 1.

(17) Cheng, Y.-H.; Zhao, X.; Song, K.-S.; Liu, L.; Guo, Q.-X. *J. Org. Chem.* **2002**, *67*, 6638.

(18) Song, K.-S.; Liu, L.; Guo, Q.-X. *J. Org. Chem.* **2003**, *68*, 262.

(19) SYBYL 6.7, *Molecular Modelling Software*; TRIPOS, Inc.: St. Louis, MO, 2001.

(20) Stewart, J. J. P. *J. Comput. Chem.* **1989**, *10*, 221.

(21) Stewart, J. J. P. *MOPAC 7.0, A Public-Domain General Molecular Orbital Package*; Frank J. Seiler Research Laboratory, US Air Force Academy: Colorado Springs, CO, 1993.

**Acknowledgment.** Two of the authors (F.F. and K.P.) wish to express their gratitude to the Research Council for Natural Sciences, The Academy of Finland, and to the National Scientific Research Grant, Hungary (T 4466), for financial support.

**Supporting Information Available:** Analytical data on compounds of series **12** (Table S1);  $^{13}\text{C}$  and  $^{15}\text{N}$  NMR data and

PM3 atomic charges for series **7**, **10**, **12–14** (Tables S2–S6); bond lengths in Table S7;  $\delta_{\text{N}}(\text{C}=\text{N})$  vs  $\sigma$  correlation for series **10** (Figure S1);  $\delta_{\text{N}}(\text{N}2)$  vs  $\sigma$  correlation for series **10** (Figure S2);  $q_{\text{N}}(\text{N}2)$  vs  $q_{\text{C}}(\text{C}=\text{N})$  correlation for series **7** (Figure S3); and  $\delta_{\text{C}}(\text{C}=\text{N})$  vs  $q_{\text{C}}(\text{C}=\text{N})$  correlation for series **7** (Figure S4). This material is available free of charge via the Internet at <http://pubs.acs.org>.

JO020608L